© 2014. Published by The Company of Biologists Ltd | Development (2014) 141, 674-684 doi:10.1242/dev.100107

RESEARCH ARTICLE

Multiple developmental mechanisms regulate species-specific jaw size

Jennifer L. Fish, Rachel S. Sklar, Katherine C. Woronowicz and Richard A. Schneider*

ABSTRACT

Variation in jaw size during evolution has been crucial for the adaptive radiation of vertebrates, yet variation in jaw size during development is often associated with disease. To test the hypothesis that early developmental events regulating neural crest (NC) progenitors contribute to species-specific differences in size, we investigated mechanisms through which two avian species, duck and quail, achieve their remarkably different jaw size. At early stages, duck exhibit an anterior shift in brain regionalization yielding a shorter, broader, midbrain. We find no significant difference in the total number of pre-migratory NC; however, duck concentrate their pre-migratory NC in the midbrain, which contributes to an increase in size of the post-migratory NC population allocated to the mandibular arch. Subsequent differences in proliferation lead to a progressive increase in size of the duck mandibular arch relative to that of quail. To test the role of pre-migratory NC progenitor number in regulating jaw size, we reduced and augmented NC progenitors. In contrast to previous reports of regeneration by NC precursors, we find that neural fold extirpation results in a loss of NC precursors. Despite this reduction in their numbers, post-migratory NC progenitors compensate, producing a symmetric and normal-sized jaw. Our results suggest that evolutionary modification of multiple aspects of NC cell biology, including NC allocation within the jaw primordia and NC-mediated proliferation, have been important to the evolution of jaw size. Furthermore, our finding of NC post-migratory compensatory mechanisms potentially extends the developmental time frame for treatments of disease or injury associated with NC progenitor loss.

KEY WORDS: Species-specific jaw size, Cranial neural crest, Evolution of development, Quail-duck chimeras

INTRODUCTION

Developmental variation in jaw size can cause severe, often life threatening, defects. However, variation in jaw size has also been crucial to the evolution and adaptation of vertebrates. Therefore, understanding how jaw size is regulated during development, and how species-specific variation is achieved, is important for studies of both disease and evolution. Differences in size have long been noted as essential for many components of organismal function, but the mechanisms by which development properly regulates size remain elusive (Haldane, 1927). Experiments in tissue regeneration and transplantation strongly suggest that organs have an intrinsic mechanism enabling them to know their proper size and to regulate growth accordingly (Leevers and McNeill, 2005). However, how intrinsic cellular programs normally operate within the environment of the tissue to inhibit growth remains poorly understood. Nor is it clear what mechanisms might be subject to evolutionary modification upon selection for a change in organ size.

We approached these questions by investigating mechanisms through which two avian species, quail and duck, achieve their remarkably different jaw size (Fig. 1A). In particular, we focus on the lower jaw skeleton, which arises from the paired mandibular primordia. Neural crest (NC) cells that migrate out of the caudal midbrain and rostral hindbrain are the only source of skeletogenic mesenchyme within the mandibular primordia (Couly et al., 1993; Köntges and Lumsden, 1996; Le Lièvre and Douarin, 1975; Noden, 1978; Noden and Schneider, 2006). Previous work has shown that the orchestration of developmental programs regulating jaw size is under the regulatory control of NC (Eames and Schneider, 2008; Jheon and Schneider, 2009; Schneider, 2005; Schneider and Helms, 2003; Tokita and Schneider, 2009), but how NC achieves this complex task remains unclear.

NC formation involves a multi-step regulatory process, beginning with induction at the border of the neural and non-neural ectoderm, specification in the dorsal neural tube, maintenance of multi-potency and cell cycle control, and finally delamination and migration (Betancur et al., 2010; Sauka-Spengler and Bronner-Fraser, 2008). NC cells that migrate out of the midbrain and first and second rhombomeres of the hindbrain populate the mandibular primordia (Couly et al., 1993; Köntges and Lumsden, 1996; Le Lièvre and Douarin, 1975; Noden, 1978). Although the gene networks orchestrating these processes appear to be highly conserved across vertebrates, reflecting a fundamental adaptation of the new head (Bronner-Fraser, 2008; Depew and Olsson, 2008; Nikitina et al., 2008; Glenn Northcutt, 2005), much remains to be understood about how diversity in the size and shape of NC derivatives is achieved. Given the emphasis in the literature on the ability of NC to regenerate, NC progenitor number is assumed to be crucial to proper regulation of size. Here, we investigated the role of early developmental events that establish NC progenitor number, regulate proliferation and ultimately determine jaw size.

To test the hypothesis that differences in NC progenitor number and proliferation rates contribute to species-specific differences in jaw size, we investigated the cell biology of NC in quail and duck embryos at multiple key developmental phases (Table 1). Our results suggest that evolutionary modification of multiple aspects of NC cell biology, including NC allocation within the jaw primordia and NC-mediated proliferation dynamics, have been important to the evolution of large jaw size. We also tested the role of NC progenitor number in determining mandible size by reducing and augmenting NC progenitors, neither of which had a significant effect on size. Our data indicate that normal jaw size is achieved after NC progenitor reduction by local regulation of proliferation within the post-migratory environment of the mandibular arch. Regulative development in the local environment of the mandibular arch allows for compensation of NC lost as a result of damage or disease, which

University of California, 513 Parnassus Ave, S-1159 San Francisco, CA 94143, USA.

*Author for correspondence (rich.schneider@ucsf.edu)

Received 14 June 2013; Accepted 15 November 2013

Development (2014) doi:10.1242/dev.100107

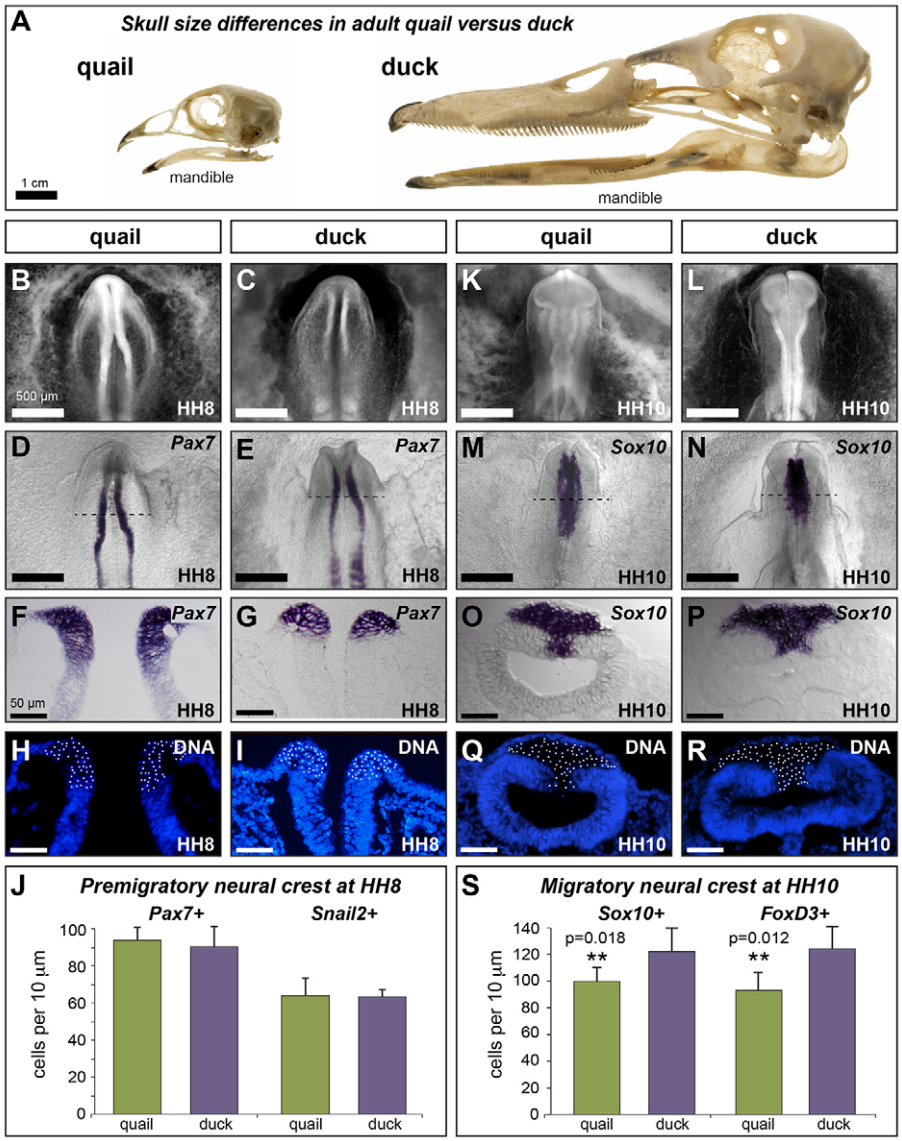

Fig. 1. Species-specific differences emerge progressively during development. (A) Adult quail and duck skulls showing species-specific differences in jaw size, highlighted by the mandible. (B,C) Ethidium bromide staining of HH8 quail and duck embryos. (D-G) *In situ* hybridization (ISH) for *Pax7* in HH8 quail (D,F) and duck (E,G) embryos. (H,I) Cross-sections of quail (H) and duck (I) *Pax7* ISH embryos counter-stained to identify cell nuclei. (J) Quantification of *Pax7*-positive (quail: 93.8±6.9; duck: 90.3±11.1; P=0.34; n=4) and *Snail2*-positive (quail: 63.5±11.7; duck: 62.9±3.2; P=0.93; n=4) NC progenitors at HH8. (K,L) Ethidium bromide staining of HH10 quail and duck embryos. (M-P) ISH for *Sox10* in HH10 (M,O) quail and (N,P) duck embryos. (Q,R) Cross-sections of quail (Q) and duck (R) *Sox10* ISH embryos counter-stained to identify cell nuclei. (S) Quantification of *Sox10*-positive (quail: 96.4±4.1; duck: 121.1±9.5; $^{**}P$=0.018; n=3) and *FoxD3*-positive (quail: 91.0±8.1; duck: 121.8±9.1; $^{**}P$=0.012; n=3) delaminated NC progenitors in the midbrain at HH10. Scale bar measurement in B applies to B-N and that in F applies to F-R. Error bars represent s.d.

has important implications for novel treatment and recovery from congenital craniofacial disorders.

RESULTS

Pre-migratory NC progenitor population size is similar in duck and quail

To compare the size of the total multi-potent NC progenitor population in quail and duck embryos, we quantified the size of the pre-migratory NC progenitor population at the onset of NC specification in Hamburger and Hamilton (HH) stage 8 embryos and at delamination in HH10 embryos. Cells specified as NC were identified in HH8 embryos by the presence of *Pax7* and *Snail2* expression. *Pax7* is among the earliest markers of NC progenitors in vertebrates (Basch et al., 2006; Betters et al., 2010; Maczkowiak et al., 2010; Murdoch et al., 2012), and is required for NC specification in avians (Basch et al., 2006). *Snail2* has also been implicated in NC induction (LaBonne and Bronner-Fraser, 2000; Nieto et al., 1994). At HH8, quail and duck embryos are similar in size, but already distinct in head morphology (Fig. 1B-E). Nonetheless, in both species, *Pax7* and *Snail2* expression are restricted to the dorsal neural tube (Fig. 1F,G; supplementary material Fig. S1A-D) with *Snail2*-positive cells nested within an ~30% larger domain of *Pax7*-positive cells. We quantified *Pax7*- and *Snail2*-positive nuclei along the dorsal-ventral axis of quail and duck embryos and found no difference in the number (Fig. 1J; *Pax7*: quail, 93.8±6.9; duck, 90.3±11.1; P=0.34; n=4; *Snail2*: quail, 63.5±11.7; duck, 62.9±3.2; P=0.93; n=4).

Delaminated NC was identified in HH10 embryos by the presence of *Sox10* and *FoxD3* expression. Both *Sox10* and *FoxD3* are involved in the early segregation of NC from the neuroepithelium and are required for the maintenance and survival of NC during migration (Dutton et al., 2001; Kos et al., 2001; Mollaaghababa and Pavan, 2003; Teng et al., 2008). At HH10, quail and duck are still very similar in overall size, but their heads are increasingly distinct in morphology (Fig. 1K-N). Notably, the midbrain in duck is shorter and broader than in quail. This difference in morphology is mirrored by differences in the *Sox10* expression domain, which is broader in the midbrain of duck, but has a reduced posterior extent relative to quail (Fig. 1M,N). A similar pattern was found for *FoxD3* (supplementary material Fig. S1G,H). Although *Sox10* and *FoxD3* are expressed in different sub-populations of differentiating neural crest later in development, at HH10, all delaminated, mesenchymal

Development (2014) doi:10.1242/dev.100107

Table 1. Development of mandibular arch neural crest in quail versus duck

Stage	Time (approximate hours)		Developmental phase	Assay performed
	Quail	Duck		
HH8	30	44	Pre-migratory progenitors	*Pax7*/*Snail2* ISH
HH10	36	62	Delaminated progenitors	*Sox10*/*FoxD3* ISH
HH13	44	87	Post-migratory allocation	*Dlx2* ISH
HH16	60	108	Proliferation	PH3 immunostaining
HH20	76	132	Proliferation	BrdU incorporation

cells express both *Sox10* and *FoxD3*, whereas stratified cells of the neuroepithelium are negative (Fig. 1O,P; supplementary material Fig. S1I,J). Quantification of *Sox10*- and *FoxD3*-positive cells mirror this co-expression, both revealing that duck have ~20% more delaminated NC in the midbrain than do quail (Fig. 1S; *Sox10*: quail, 96.4±4.1; duck, 121.1±9.5; P=0.018; n=3; *FoxD3*: quail, 91.0±8.1; duck, 121.8±9.1; P=0.012; n=3).

The observation of distinct head morphology and differently sized *Sox10* expression domains in HH10 quail and duck embryos suggested that differences in anterior-posterior patterning of the brain (in addition to dorsal-ventral patterning of the neural tube) might also influence pre-migratory NC progenitor number. We therefore also evaluated anterior-posterior patterning of the brain in quail and duck embryos using several well-established markers of brain regionalization: *FoxG1* (anterior forebrain), *Pax6* (forebrain), *Otx2* (fore- and midbrain), *Fgf8* (midbrain-hindbrain boundary) and *Krox20* [rhombomere (R) 3 and R5 of the hindbrain]. Although *FoxG1* expression is similar in quail and duck (Fig. 2A,B), *Pax6* expression in the presumptive forebrain occupies a slightly shorter domain along the anterior-posterior axis in duck (Fig. 2C,D). Expression of both *Otx2* and *Fgf8* extends more posteriorly in quail than in duck (Fig. 2E-H). *Otx2* expression in duck is not only more anteriorly restricted than in quail, but is also broader in the midbrain, highlighting the different midbrain morphology in these two species. Finally, in duck, *Krox20* expression in R3 is anterior to the developing aortic arch (Fig. 2J), whereas in quail, *Krox20* in both

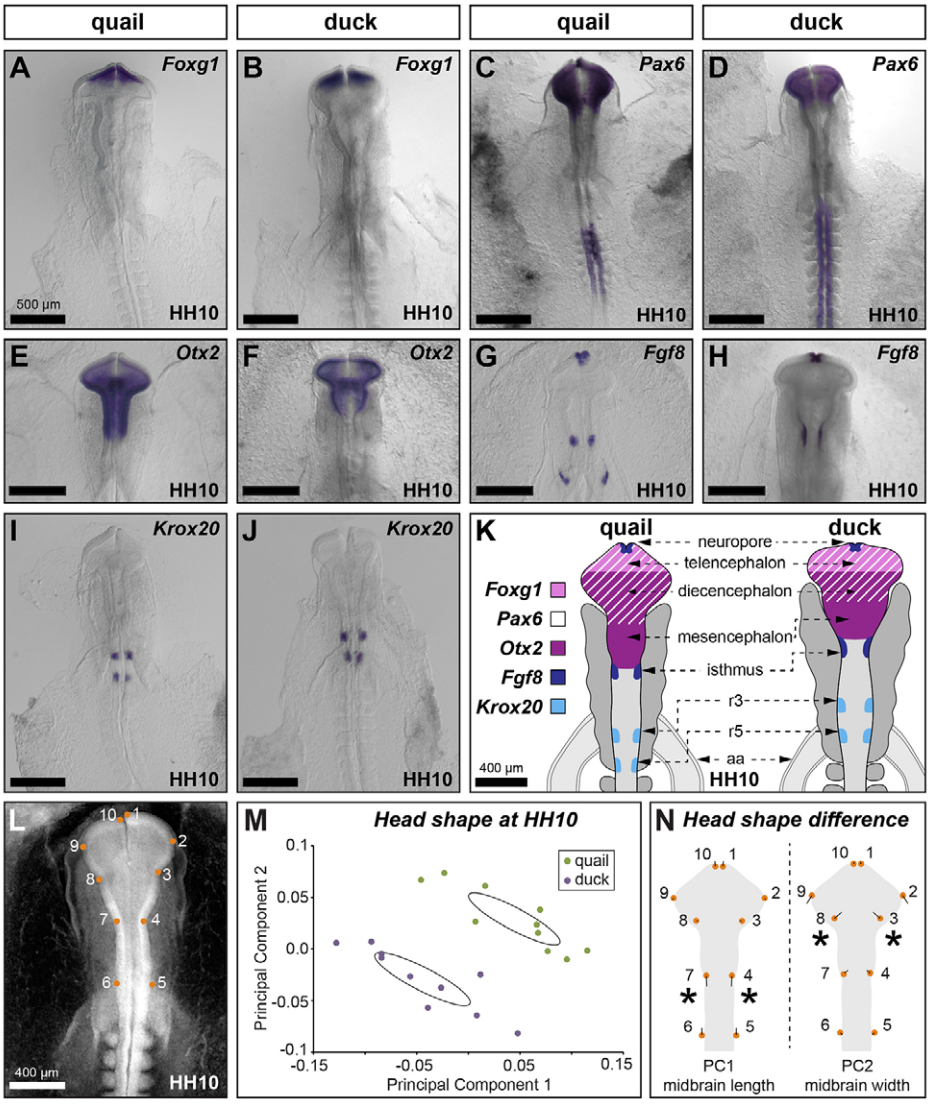

Fig. 2. Quail and duck exhibit species-specific brain regionalization. (A-J) *In situ* hybridization for *Foxg1* (A,B), *Pax6* (C,D), *Otx2* (E,F), *Fgf8* (G,H) and *Krox20* (I,J) at HH10. (K) Differences in brain regionalization between quail and duck embryos are schematized. aa, aortic arch; r, rhombomere. (L-N) Principal component analysis of head shape. (L) 2D images of HH10 embryos were analyzed with ten landmarks. Quail (green circles) and duck (purple circles) have distinct head shapes (M), with duck distinguished by an anteriorly shortened and medial-laterally broader midbrain relative to quail (N). Asterisks indicate landmarks showing the largest difference between species for each principal component. Scale bar measurement in A applies to A-J.

Development (2014) doi:10.1242/dev.100107

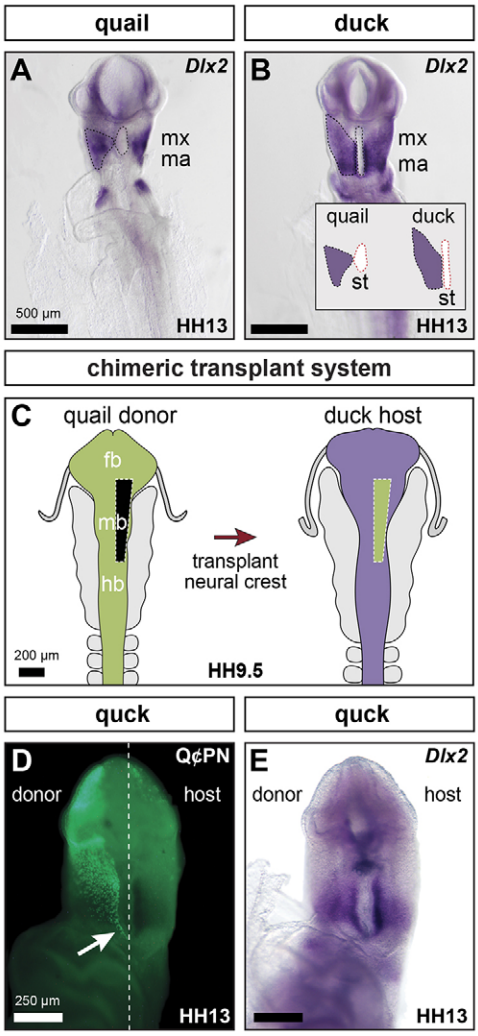

Fig. 3. Species-specific neural crest allocation. (A,B) I*n situ* hybridization for *Dlx2* at HH13 in quail (A) and duck (B) embryos. The *Dlx2*-positive NC domain is outlined with black dashed lines and the stomodeum is highlighted with red dashed lines (inset in B). (C) Experimental design for generating chimeric quck embryos. (D) Qɣ PN staining identifies nuclei of the donor quail neural crest that have migrated into the host mandibular arch. Arrow indicates the caudal extent of NC migration. (E) *Dlx2 in situ* hybridization of HH13 quck embryos is similar on both donor and host sides of the stomodeum. fb, forebrain; hb, hindbrain; mb, midbrain; md, mandible; mx, maxilla; st, stomodeum.

R3 and R5 is posterior to the developing aortic arch (Fig. 2I). This difference is independent of the position of the aortic arch, which is equidistant from the neuropore in both species (Fig. 2I,J). In sum, our molecular analysis indicates that duck exhibit an anterior shift in brain regionalization (Fig. 2K).

To quantify the morphological differences in duck and quail head shape more precisely, we performed a principal component analysis (PCA) on landmarks derived from 2D images of HH10 embryos. Head shape was estimated using ten landmarks designed to capture morphological boundaries of the three major brain vesicles and their position relative to the aortic arch (Fig. 2L). Consistent with our molecular data, PCA of HH10 embryos identifies distinct head shapes of duck and quail, exemplified by the shorter, broader midbrain in duck (Fig. 2M,N). Taken together, the molecular and morphological data indicate an evolutionary divergence in head morphology between duck and quail. Relative to quail, duck embryos have a brain that is compressed along the anterior-posterior axis, especially at the midbrain. However, duck embryos appear to maintain an equivalent total area of neural tube as quail by broadening their midbrain. In other words, the quail rostral neural tube is longer and narrower whereas the duck rostral neural tube is shorter and wider.

Species-specific differences in mandibular arch size arise during early development

To evaluate the size of the subpopulation of the total pre-migratory NC progenitor population allocated to the jaw primordia, we investigated *Dlx2* in the nascent mandibular arch. *Dlx2* is expressed by NC mesenchyme of the mandibular arch where it is important for proper dorsal-ventral patterning of the jaw (Depew et al., 2002; Jeong et al., 2008). At HH13, *Dlx2* expression is distinct in size and shape in quail and duck (Fig. 3A,B). Notably, the mandibular arch of duck is larger than that of quail, which is exemplified by their elongated stomodeum (Fig. 3A,B, red dashed lines). An elongated stomodeum generates a larger morphological space into which NC can migrate, potentially contributing to a larger population of NC cells allocated to the mandibular arch. To test the hypothesis that the number of NC cells that migrate into the mandibular arch is a consequence of the size of the available space lateral to the stomodeum, we generated chimeric ‘quck’ embryos, in which quail NC from stage-matched HH9.5 embryos was transplanted into duck embryos (Fig. 3C).

In quck, quail NC cells migrate into the mandibular arch of the duck host, where they will ultimately form a mandible that is quail-like in size and shape (Eames and Schneider, 2008; Schneider and Helms, 2003). We evaluated the distribution of quail NC in HH13 quck by immunostaining for the quail-specific nuclear antibody Qɣ PN. Quck maintain the elongated, narrow stomodeal morphology of the duck host (Fig. 3D,E). Within this host environment, quail NC cells migrate into the mandibular arch, filling the space along the entire length of the stomodeum in a duck-like pattern (Fig. 3D). Additionally, at very early stages, the size and shape of the *Dlx2*-positive NC domain in the mandibular arch is similar on the host and donor sides of the stomodeum (Fig. 3E; n=6). These data suggest that morphological boundaries defined by the stomodeum affect the size of the post-migratory NC population allocated to the mandibular arch.

Species-specific differences in mandibular arch size develop progressively

As the mandibular arch grows from HH13 to HH20, the difference in size between duck and quail progressively increases (Fig. 4A-D). By HH16, the duck mandibular arch is visibly larger than that of quail (Fig. 4A,B,E,F), and continues to grow in relative size at HH20 (Fig. 4C,D). To quantify this difference in size, we isolated mesenchyme from HH20 mandibles and found that duck have approximately twice as many cells as quail (Fig. 4H; quail: 131,553±8,042; duck, 249,953±5,856; P<0.0001; n=4). We examined proliferation of mandibular mesenchyme by two separate methods. First, we quantified the number of proliferating cells at HH16 and HH20 by counting Phosphohistone H3 (PH3)-positive cells (Fig. 4E-G). We observed no difference in relative number of proliferating cells in duck and quail mandibular mesenchyme at either HH16 or HH20 (Fig. 4G). We next investigated the rate at which mandibular mesenchyme proliferates using a bromodeoxyuridine (BrdU)/iododeoxyuridine (IdU) pulse-chase paradigm in HH20 embryos (Fig. 4I-L). The length of the S phase

Development (2014) doi:10.1242/dev.100107

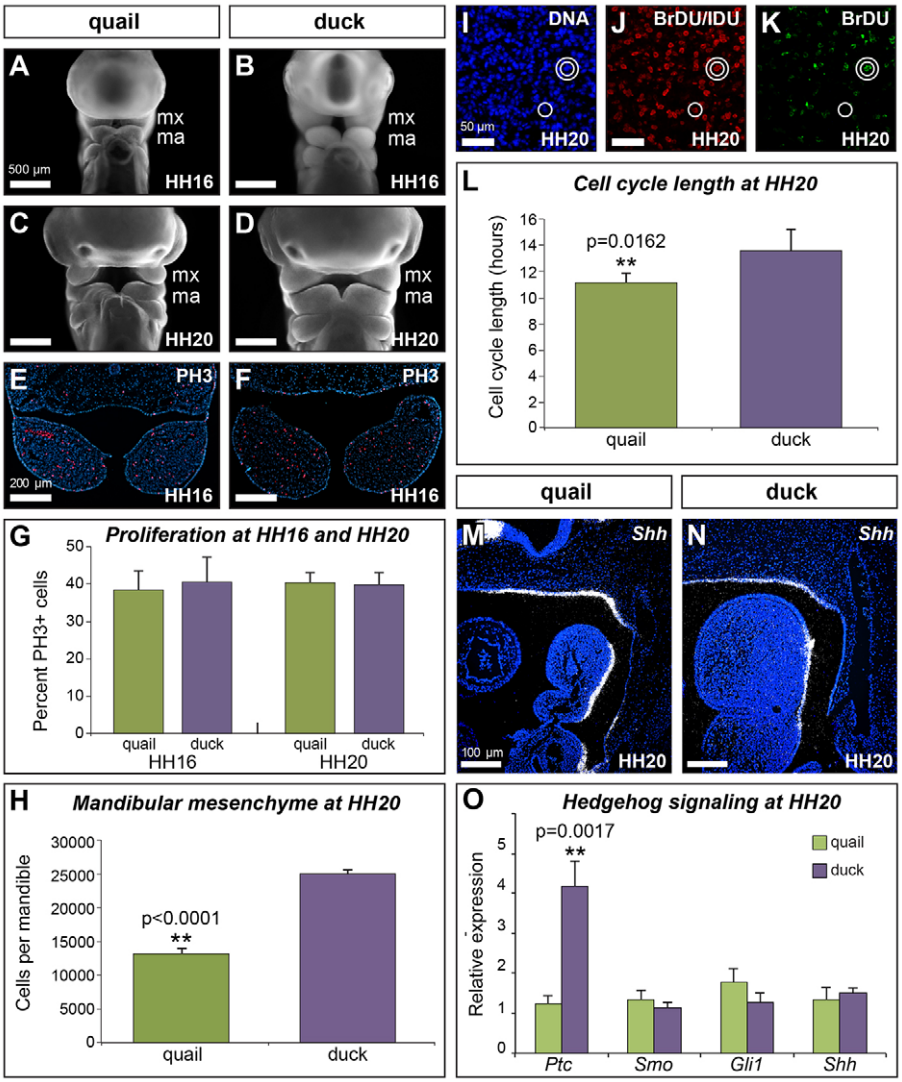

Fig. 4. Growth and proliferation of the mandibular arch. (A-D) Ethidium bromide staining at HH16 and HH20 of quail (A,C) and duck (B,D) embryos. (E,F) Immunostaining for phosphohistone H3 (PH3) identifies mitotic cells in HH16 quail (E) and duck (F) embryos. (G) Quantification of PH3-positive cells in HH16 and HH20 duck and quail embryos (quail HH16: 38±4.7%; quail HH20: 40.3±3.1%; duck HH16: 41.8±5.5%; duck HH20: 41.2±3.5%; n=3). (H) By HH20, duck have approximately twice as many cells as quail in the mandibular arch (quail: 131,553±8042; duck: 249,953±5856; **P<0.0001; n=4). (I-K) Sections of HH20 mandibular arches show Hoescht staining for cell nuclei (I), immunostaining for BrdU and IdU to identify double-labeled cells (double white circles) (J), and immunostaining for BrdU only to identify single-labeled cells (single white circle) (K). (L) Quantification of the cell cycle in quail and duck mandibular mesenchyme at HH20 (quail: 11.0±0.8 hours; duck: 13.5±1.6 hours; **P=0.0162; n=5 per species). (M,N) Sagittal sections of HH20 quail (M) and duck (N) embryos, showing sonic hedgehog expression (Shh) in the pharyngeal endoderm. (O) Relative expression of genes involved in the Shh pathway in HH20 mandibles (n=3). Error bars represent s.d.

(T_S) and the total length of the cell cycle (T_C) were determined based on the ratio of the total number of cells (Fig. 4I) that incorporated both (Fig. 4J, double circle) or one (Fig. 4K, single circle) of the thymidine analogs (Martynoga et al., 2005; Siegenthaler et al., 2008). As the relative number of proliferating cells is equivalent in duck and quail HH20 mandibular mesenchyme, any difference in the number of double- or single-labeled cells is inferred to reflect differences in T_S or T_C. We found that the cell cycle of mandibular mesenchyme is ~20% faster in quail than in duck (Fig. 4L; 11.0±0.8 hours compared with 13.5±1.6 hours; P=0.0162; n=5).

The fact that the duck mandibular arch progressively increases in relative size compared with the quail whereas the mandibular mesenchyme of duck is cycling more slowly than that of quail is initially counter-intuitive. However, duck are also developing at a slower rate over this time interval, taking ~45 hours to progress from HH13 to HH20, whereas quail average only 32 hours (Table 1). Therefore, duck mandibular mesenchyme completes ~3.3 cycles during this developmental window compared with an average of 2.9 cycles for quail. Thus, the rate of proliferation relative to the rate of development is faster in duck mandibular mesenchyme than in quail mandibular mesenchyme. As a consequence, a small difference in the size of the subpopulation of NC cells allocated to the mandibular arch at HH13 (e.g. a 15% increase, or a difference of 1.15 to 1), translates into a twofold difference in size (e.g. 7.46 to 15.62) by HH20 (Table 2).

Previously, sonic hedgehog (Shh) has been shown to regulate growth and proliferation of the mandibular arch (Brito et al., 2008; Roper et al., 2009; ten Berge et al., 2001). We have observed that *Shh* is expressed in similar domains in duck and quail embryos (Fig. 4M,N). However, we hypothesized that one mechanism mediating differences in species-specific rates of proliferation could

Table 2. Proliferation dynamics of mandibular arch NC from HH13 to HH20

Measurement	Quail	Duck
Relative population size at HH13	1	1.15
Absolute time from HH13 to HH20	32 hours	45 hours
Cell cycle length	11 hours	13.5 hours
Number of cycles from HH13 to HH20	2.9	3.3
Doubling equation	$(1.00)2^{2.9}$	$(1.15)2^{3.3}$
Relative population size at HH20	7.46	15.62

When accounting for differences in developmental rate and NC proliferation, a 15% increase in NC population size at HH13 in duck embryos becomes a twofold difference in NC number by HH20.

Development (2014) doi:10.1242/dev.100107

be differential regulation of, or response to, Shh signaling. To test this, we quantified relative expression of several genes involved in the Shh signaling pathway, including *Ptc*, *Smo* and *Gli1* in quail versus duck. We found that whereas *Smo*, *Gli1* and *Shh* are expressed at similar levels, *Ptc* is approximately four times higher in duck than quail (Fig. 4O; P=0.0017). Thus, quail and duck mandibular mesenchyme differ in their regulation of genes involved in the Shh pathway.

Neural crest exhibits compensatory behavior

Surprisingly, we did not find a difference in the initial size of the total pre-migratory NC progenitor population in duck and quail (Fig. 1), suggesting that the size of the pre-migratory NC progenitor population is not a crucial regulator of jaw size. To test this hypothesis, we either reduced pre-migratory NC progenitor numbers in HH9– embryos by partial unilateral neural fold extirpation (Fig. 5A) or augmented their numbers by neural fold transplantation from a GFP-positive donor to a GFP-negative host (Fig. 5B).

To show that extirpation reduces NC cell number, embryos were collected 4 to 12 hours (corresponding to stages HH9+ to HH10) after surgery. The extent of re-specification of the dorsal neural tube representing local regeneration of NC progenitors was examined by *in situ* hybridization for *Pax7* on HH9+ embryos (up to 6 hours post-surgery). In all cases, we observed an absence of *Pax7* expression in the surgically manipulated area (Fig. 5C; n=12). The effect of neural fold extirpation on the number of delaminated and migrating NC progenitors was examined with *Sox10 in situ* hybridization on HH9.5-10 embryos (8-12 hours post-extirpation). In all cases, we observed a reduction of *Sox10*-positive migrating NC (Fig. 5D,E; n=11). Unoperated sides of extirpated embryos exhibit *Sox10*-positive cells migrating away from the neural tube (Fig. 5E,F, arrows); however, surgically manipulated sides lack migrating cells in the contralateral region (Fig. 5E,F, asterisks). Thus, neural fold extirpation results not only in the absence of NC marker gene expression, but also reduces the number of migrating NC cells. In embryos analyzed at HH13 (n=4), we observed smaller domains of *Dlx2* expression in the NC of the mandible on the extirpated side compared with the unoperated side (Fig. 5G, asterisk).

Observations of gross morphology of HH38 embryos revealed that neither NC progenitor reduction (Fig. 5H; n=9) nor augmentation (Fig. 5I; n=6) has a significant effect on jaw size or symmetry relative to control embryos. Quantitative analyses were performed on isolated mandibles from embryos processed for differential skeletal staining (Fig. 5J). Jaw symmetry was evaluated by comparing right (experimentally manipulated) and left (internal control) sides of the mandible in extirpated, augmented and control embryos. No significant difference in the size of the right versus left side of the mandible was found, with average ratios approximating 1.0 for all three conditions (Fig. 5K). We also directly evaluated absolute size by comparing the average length of the right (experimentally manipulated) side of the mandible in extirpated embryos with the average length of the right side of the mandible in control embryos. No significant difference was found in the absolute length of the mandible when NC progenitor number was reduced by neural fold extirpation (Fig. 5K).

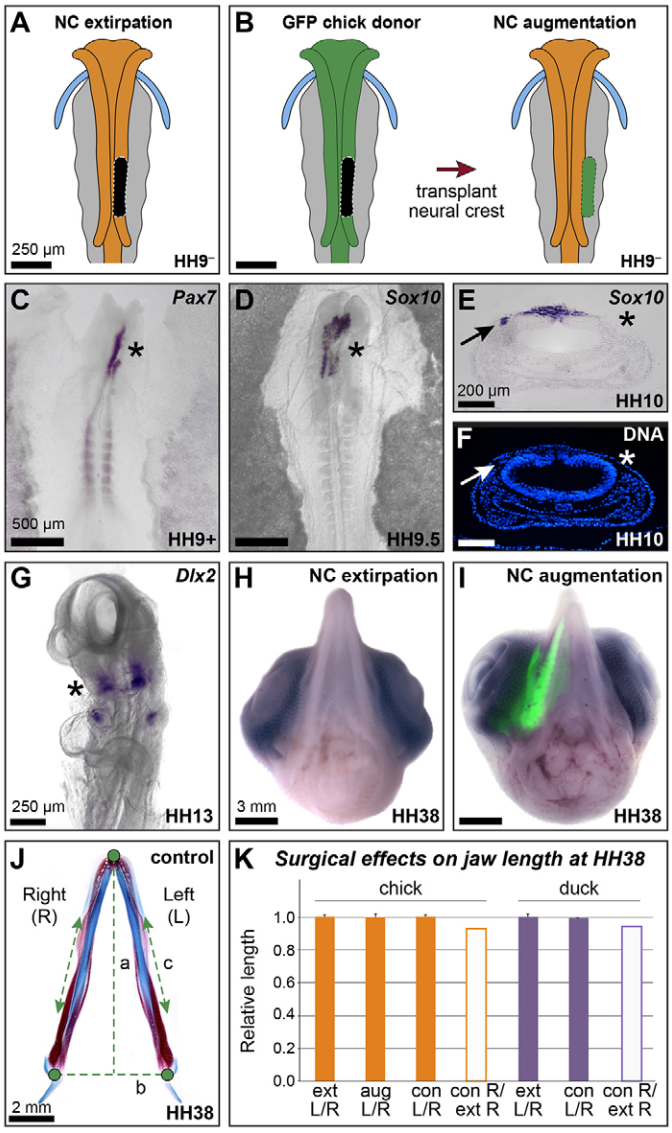

Fig. 5. Neural crest exhibits compensatory behavior. (A) Strategy for reducing neural crest progenitor number by neural fold extirpation. Black area indicates area of extirpated neural fold. (B) Strategy for augmenting neural crest progenitor number by neural fold transplantation. (C) *Pax7 in situ* hybridization in HH9+ embryos (4 hours post-extirpation; n=12). (D) *Sox10 in situ* hybridization in HH9.5-10 embryos (6-8 hours post-extirpation; n=11). Asterisks in C,D highlight reduction in gene expression on extirpated side. (E,F) Cross-section of *Sox10* ISH embryo at HH10 counter-stained with Hoechst. Arrows identify *Sox10*-positive migrating NC cells on the control, unoperated side. Asterisks highlight the absence of migrating NC and *Sox10* expression on the extirpated side. (G) Ventral view of *Dlx2* in an HH13 embryo, showing reduced expression on extirpated side (asterisk) (n=4). (H,I) Ventral views of unilateral neural fold extirpation (H; n=9) and unilateral GFP neural fold augmentation (I; n=6) chick at HH38. (J) Strategy for quantifying mandible length at HH38 (see Materials and Methods). (K) Quantification of jaw length in control (con), extirpated (ext) and augmented (aug) chick and duck at HH38. Error bars represent s.d.

Species-specific patterns of gene expression precede and predict species-specific morphological differences

Because the earliest difference in mandible size in duck and quail appears to correspond to a change in anterior-posterior patterning of the brain, we investigated anterior-posterior patterning of the neural plate in duck and quail to determine when during development this difference first appears. Mirroring the overall similarity in embryo size (Fig. 6A,B), we found that the length of the anterior half of the embryo from Henson's node to the prechordal plate, where *Shh* is expressed, is equivalent in the two species (Fig. 6C,D). Similarly, the overall length of *Fgf8* expression in the primitive streak indicates

Development (2014) doi:10.1242/dev.100107

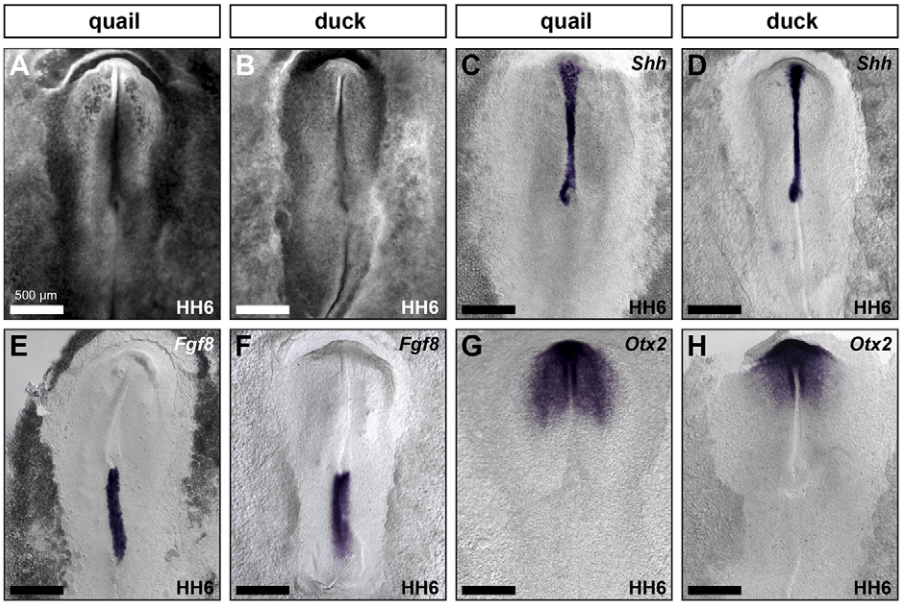

Fig. 6. Species-specific jaw size appears early during development. (A-H) HH6 quail and duck stained with ethidium bromide (A,B), and *Shh* (C,D), *Fgf8* (E,F) and *Otx2* (G,H) *in situ* hybridization. Scale bar measurement in A applies to A-H.

that size of the posterior domain of the embryo is not significantly different in these two species (Fig. 6E,F). By contrast, the *Otx2* expression domain is distinct in quail and duck, showing a greater posterior extension in quail than in duck (Fig. 6G,H), presaging the differences in gene expression and morphology observed in HH10 embryos (Fig. 3E,F).

DISCUSSION

Developmental and cellular origins of species-specific jaw size

Our quantitative analyses indicate that species-specific differences in mandibular arch size arise progressively during development. Initially, the total pre-migratory NC progenitor population at HH8 (expressing *Pax7* or *Snail2*) in duck and quail is equivalent in size. Although the possibility exists that the size of the pre-migratory NC progenitor population could be subject to evolutionary modification (Li et al., 2009; Steventon and Mayor, 2012; Yardley and García-Castro, 2012), we do not observe such differences between quail and duck. Instead, our data suggest that at least three other developmental events contribute to species-specific differences in size (Fig. 7). First, differences in the anterior-posterior patterning of the neural plate establish distinct brain domains, ultimately generating a shorter and wider midbrain in duck. Second, duck embryos exhibit a larger allocation of post-migratory NC progenitors to the jaw primordia. Third, duck mandibular mesenchyme exhibits increased proliferation relative to quail mandibular mesenchyme.

The earliest event, that affecting neural plate patterning, may have multiple effects on jaw size. The stomodeum arises between the infundibulum of the diencephalon and the developing aortic arch (Gilbert, 2010; Pikalow et al., 1994; Shigetani et al., 2000; Withington et al., 2001). Therefore, the elongated stomodeum of duck may be a consequence of the anterior shift in brain regionalization. In quck embryos, we found that quail donor NC cells are distributed in the duck host mandibular arch in a duck-like pattern (Fig. 3D,E), suggesting that the size of the NC population allocated to the mandibular arch is due in part to a space-filling event. Thus, the larger number of NC cells allocated to the mandibular arch in duck may derive from two phenomena that are consequences of alterations to neural plate patterning. First, the anterior shift generates a wider midbrain that increases the number of NC cells delaminating from the posterior midbrain, effectively concentrating NC in a migratory pathway directed towards the mandibular arch. Second, the anterior shift increases the size of the mandibular arch domain, allowing more NC to fill the area around the stomodeum.

We find that species-specific differences in size are related to the number of NC cells that migrate into the mandibular arch, followed by differences in NC proliferation. Interestingly, alterations to these mechanisms have also been implicated in craniofacial anomalies. In particular, Treacher-Collins syndrome, which is characterized by hypoplasia of the mid and upper face and cheek bones, is caused by an abnormal deficiency in migrating NC and reduced rates of NC proliferation (Dixon et al., 2006). These data suggest that the same developmental mechanisms that are disrupted during disease may be targeted in evolution.

Evolution of morphology and development

Two distinct models dominate explanations of the relationship of developmental processes to morphological change. A ‘funnel’ model argues that embryos show the greatest morphological conservation early in development, followed by morphological diversification at later stages (Arthur, 1984; von Baer, 1828; de Beer, 1940; Riedl, 1978). By contrast, the ‘hourglass’ model emphasizes morphological conservation at organogenesis, which is called the phylotypic period (Duboule, 1994; Irie and Kuratani, 2011; Rudolf, 1996). In avians, the phylotypic period corresponds roughly to stage HH16 (Irie and Kuratani, 2011).

Previous reports comparing pigeon and chick embryos argued that early-stage avian embryos are indistinguishable from each other and that species-specific differences in craniofacial morphology only start to appear at the phylotypic period (Helms and Brugmann, 2007; Liu et al., 2010). By contrast, our data indicate that, from their earliest appearances, the neural tube and mandibular arch are morphologically distinct in quail and duck embryos (Figs 1, 2). The developmental basis for this distinct morphology, alteration to neural plate patterning, is already apparent at HH6, and probably originates prior to gastrulation. Thus, overt species-specific differences in gene

Development (2014) doi:10.1242/dev.100107

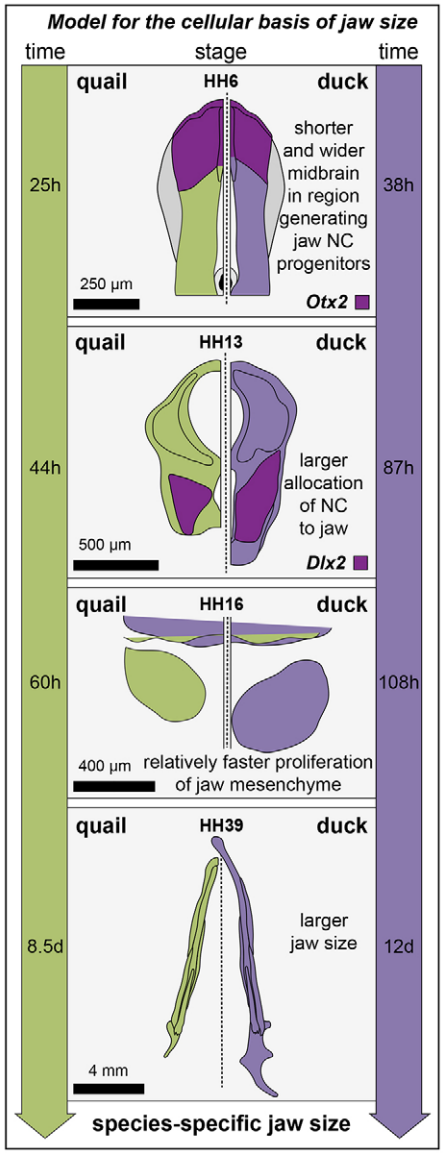

Fig. 7. Model for the cellular basis of jaw size. Specification of the neural plate establishes the basis for a shorter and wider midbrain in the region generating jaw NC precursors in duck embryos (event 1). This difference, represented by distinct *Otx2* expression domains, is evident by HH6. The wider midbrain of duck contributes to a larger allocation of NC to the jaw primordia in HH13 embryos (event 2). NC cells of the duck jaw mesenchyme exhibit an increase in proliferation compared with quail. Increased proliferation (event 3) is driven largely by differences in developmental rate (see time scale on the side of the diagrams). Thus, the larger jaw size of duck is the result of at least three distinct developmental events (outcome 4).

expression appear earlier in development and precede related species-specific differences in morphology.

A recent comparative transcriptome analysis of embryos of several different classes of vertebrates found that gene expression is conserved in the phylotypic stage and more divergent at earlier and later stages of development (Irie and Kuratani, 2011). Similar results from investigations of *Caenorhabditis* (Levin et al., 2012) and *Drosophila* (Kalinka et al., 2010) suggest that morphological conservation is correlated with molecular conservation. Perhaps in an effort to address issues of heterochrony, these genome-wide approaches have not identified signals of heterotopy or changes in levels of gene expression. In all of our comparisons between quail and duck, the crucial events driving differences in jaw size appear to be related to differences in the expression of the same gene. We observed a difference in the spatial expression of *Otx2* at HH6, and later at HH20 we find differences in levels of expression of genes in the Shh signaling pathway that may contribute to differential regulation of proliferation. Although genome-wide analyses have great power to identify large-scale patterns, understanding mechanisms of evolution will require more investigations of the emergent and hierarchical properties of small variations in gene expression and their downstream effects on gene regulatory networks (Betancur et al., 2010; Erwin and Davidson, 2009).

Neural crest compensation and regulation of mandibular size

Our results showing that neither reduction nor augmentation of NC progenitor numbers had a significant effect on jaw size (Fig. 5G-K) are consistent with previously reported observations of normal jaw development after neural fold extirpation (Couly et al., 1996; Hunt et al., 1995; Scherson et al., 1993; Sechrist et al., 1995). In these previous reports, however, normal jaw development was argued to result from regeneration of pre-migratory NC progenitors at the site of the neural tube, either by re-specification of the dorsal neural tube (Hunt et al., 1995; Sechrist et al., 1995) or by a doubling of migratory NC progenitors produced by the neighboring neural folds (Couly et al., 1996; Scherson et al., 1993). None of these earlier studies quantitatively evaluated NC progenitor number before or after neural fold extirpation, instead hypothesizing NC regeneration largely from observations of end-point phenotypes. Although our data do not rule out the possibility that some, albeit limited, NC regeneration may occur, we instead find that (1) neural fold extirpation significantly reduces the number of premigratory NC cells and (2) normal development of mandible size after NC progenitor reduction requires some other mechanism beyond regeneration of NC progenitors at the neural tube. One possibility is that NC cells re-populate the mandibular arch by crossing over from the contralateral side and/or by ingressing from anterior or posterior to the surgical site (Kulesa et al., 2000; Scherson et al., 1993). Importantly, we do not think that the contralateral side or neighboring tissue regenerates NC, but rather that delaminated NC cells may alter their normal migration pattern to fill the open space generated by the extirpation. This is confirmed by our analysis of embryos at HH13, which show that there are NC cells that arrive in the mandibular arch following extirpation, but their numbers are reduced as determined by the smaller size of the *Dlx2* expression domain. Moreover, any NC cells that migrate into the domain lateral to the surgical extirpation would probably do so at the expense of migrating to their normal destination. Although we did not quantify the effect of extirpation on other components of the skull, we did not see any obvious defects, suggesting that the developmental systems regulating these elements can also compensate from the loss of some progenitors. We hypothesize that NC cells compensate for reduction in progenitor numbers by cell-autonomously regulating their proliferation in the post-migratory environment of the mandibular arch. Such compensation is likely to occur very early, as we did not observe significantly different proliferation rates in mandibular arch mesenchyme of extirpated embryos versus control embryos at HH20 (data not shown).

Although our data indicate that reduction of NC progenitor number does not significantly affect mandible size, we do observe a slight reduction in mandible size of extirpated embryos at HH38.

Development (2014) doi:10.1242/dev.100107

We consider it likely that as the jaw continues to grow through later development, this slight difference may increase to significance, and that in order to achieve very large jaw size, some increase in pre-migratory NC progenitor number may be necessary.

Regulative development of the mandible

In many ways, the mandibular arch is similar to limb buds in that both rely on interactions between mesenchyme and epithelium and both employ many of the same key regulatory genes (Schneider et al., 1999). Regulation of limb size has been argued to function via a signaling feedback loop involving Shh and Fgf8, in which cellular interactions are sensitive to distance within the growth field (Allard and Tabin, 2009). We hypothesize that mandibular growth is regulated by a similar signaling feedback loop. *Shh* expression in the pharyngeal endoderm is essential for mandibular development, where it directs neural crest survival and outgrowth (Ahlgren and Bronner-Fraser, 1999; Balczerski et al., 2012; Brito et al., 2006; Brito et al., 2008; David et al., 2002; Jeong et al., 2004; Veitch et al., 1999). Exogenous Shh, when placed in the mandibular arch environment, activates *Bmp4* and *Fgf8* expression in the oral ectoderm, resulting in the development of supernumerary mandibles (Brito et al., 2008). Together, these data support the hypothesis that jaw size is reliant on proliferation within the mandibular arch environment (regulative development) rather than being entirely dependent on initial NC progenitor number (determinant development).

We have investigated cell cycle regulation with respect to osteogenic differentiation in the mandible and found that stage-matched quail and duck embryos differ in their relative expression of p27 and several cyclins (Hall et al., 2013), providing one possible mechanism for species-specific differences in cell cycle length. We also hypothesize that epithelially expressed signaling factors within the mandibular arch (such as Shh, Fgf8 and Bmp4) cooperatively stimulate proliferation within the mandible, with outgrowth progressing until the mesenchyme reaches its proper size. Species-specific differences in mandible size would then be achieved through cell-autonomous differences in the response to these signals. For example, we found a fourfold increase in the expression level of the Shh receptor *Ptc* in mesenchyme of duck embryos relative to quail at HH20 (Fig. 4O). Such distinct species-specific expression could modulate the response to Shh, and control the dynamics of proliferation and growth (Roper et al., 2009). Similarly, we have demonstrated that at slightly later stages preceding osteogenic differentiation (e.g. HH24), mandibular mesenchyme dictates when bone forms by temporally regulating its interactions with epithelium and its own expression of *Bmp4* (Merrill et al., 2008).

Developmental mechanisms that compensate for pre-migratory NC progenitor loss in the post-migratory environment of the mandibular arch may possibly extend the developmental time during which recovery from damage or disease can occur. Future research dedicated to elucidating details of these compensatory mechanisms has great potential to contribute to new biologically based therapies for craniofacial disorders, such as mandibular hypoplasias.

MATERIALS AND METHODS

Gene expression analyses

Whole-mount *in situ* hybridization (ISH) was performed following standard protocols (Depew et al., 1999). Embryos were hybridized at 65°C with digoxygenin-labeled riboprobes for chicken *Dlx2*, *Fgf8*, *Shh* (gifts of John Rubenstein, University of California, San Francisco, CA, USA), *Pax6*, *Pax7* (gifts of Andrea Streit, King's College London, UK), *FoxG1*, *FoxD3*, *Sox10*, *Krox20* (gifts of Marianne Bronner, The California Institute of Technology, CA, USA), *Otx2* (gift of Edoardo Boncinelli, University Vita-Salute, Milan, Italy) and *Snail2* (gift of Laura Gammil, University of Minnesota, MN, USA). RT-qPCR was performed as previously described (Ealba and Schneider, 2013). Primer sequences used: SHH (forward 5′-GCTGCCATTCCAGCACCTGTCT-3′; reverse 5′-AGCGCAGAT-GAAGCCCACCAAG-3′), SMO (forward 5′-ACCCCGGGCTGCTGAGT-GAG-3′; reverse 5′-AGCGATGGTCACGTTGGCCT-3′), GLI1 (forward 5′-GGGCAAGAAGCGGGCACTGT-3′; reverse 5′-CTGCCCCG-GAGGGTTCTGGT-3′), PTC (forward 5′-CCGGCAGCACCTTGACTCT-GC-3′; reverse 5′-GCTTTGCTCCCTCCCAGAAGCA-3′). Each sample was run in triplicate and normalized to RPL19 (forward 5′-ACGC-CAACTCGCGTCAGCAG-3′; reverse 5′-ATATGCCTGCCCTTCCG-GCG-3′). Fold changes were calculated using the ΔΔC(t) method (Livak and Schmittgen, 2001).

Ethidium bromide staining

Paraformaldehyde (PFA)-fixed embryos were stained with ethidium bromide diluted 1:50,000 in PBS at room temperature for one hour. After staining, embryos were imaged with TXR fluorescence (Eames and Schneider, 2005).

Cell quantification

Neural crest cells were counted on 10-µm-thick sections of embryos after whole-mount ISH. Sections were washed in PBS, counter-stained with Hoechst dye diluted 1:1000 in PBS for 20 minutes, washed in PBS and briefly rinsed in distilled water. Quantification was performed in Photoshop by overlaying brightfield images of the ISH with fluorescent images of nuclei. For each embryo, three sections were quantified and averaged, yielding an average number of NC progenitors. Mandibular mesenchyme was quantified in HH20 embryos. Mandibles were isolated and incubated with 5% trypsin at 37°C for 15 minutes to separate the epithelium. The isolated mesenchyme was transferred to 100 µl of DMEM and homogenized by pipetting until all clumps were separated into single cells. Cell number was counted using a hemocytometer.

Morphometric analysis

ImageJ was used to obtain *xy* coordinates from ten landmarks on 2D images of ethidium bromide-stained HH10 embryos (Fig. 3L). Raw landmark coordinates were averaged across the axis of symmetry and Procrustes superimposition was used to remove the effect of rotation, scale and alignment (Coppinger and Schneider, 1995; Schneider and Helms, 2003; Zelditch, 2004). Transformed shape data were regressed against normal shape-size allometry to remove the effect of size heterogeneity and the residuals were subjected to principal components analysis in MorphoJ (Klingenberg, 2011).

Proliferation analyses

Phosphohistone H3 immunostaining

PFA-fixed embryos were sectioned at 10 µm. Sections were blocked in 10% fetal calf serum in PBS for 30 minutes at room temperature and then incubated with rabbit anti-PH3 (Cell Signaling) diluted 1:300 in blocking solution for 2 hours, washed with PBS, incubated with goat anti-rabbit Cy3 (Jackson ImmunoResearch Laboratories; diluted 1:500) and Hoechst (diluted 1:1000) in blocking solution for 1 hour. The number of PH3-positive cells per unit area was quantified using ImageJ software (NIH) using the rectangular selection tool to define equivalent areas in quail and duck mandibular arches. PH3-positive cells were counted and normalized to the area of the rectangle. For each embryo, three sections were quantified and averaged, yielding an average number of PH3-positive cells/area. Species averages were generated from the averages of three embryos.

Cell cycle length calculation

Cell cycle length was calculated in quail and duck HH20 mandibular arches following a triple-labeling protocol (Martynoga et al., 2005; Siegenthaler et al., 2008). Briefly, 100 µl of IdU (Sigma #I7125, used at 23 mg/ml in 1 M NH_4OH) was injected into an intravitelline vein followed by incubation for an interval of 90 minutes (T_i). Following the interval period, 100 µl of BrdU (Invitrogen) was injected into an intravitelline vein and embryos were incubated for 20 minutes. Embryos were rapidly collected in ice-cold PBS,

fixed overnight at 4°C in PFA. Embryo sections were immunostained with primary antibodies (mouse monoclonal anti-BrdU/IdU, BD Biosciences #347580, used at 1:200; rat monoclonal anti-BrdU from Serotec #MCA2060, used at 1:100) and secondary antibodies (Jackson ImmunoResearch Laboratories goat anti-mouse Alexa Fluor 594, used at 1:500; Jackson ImmunoResearch Laboratories goat anti-rat Alexa Fluor 488, used at 1:500) and Hoescht (1:1000). Cells positive for one thymidine analog, both thymidine analogs, and all Hoescht-positive cells were counted (at least 100 cells/section were counted). For each embryo, three sections were quantified and averaged yielding an average number of labeled cells.

Generation of chimeras

Eggs from Japanese quail (*Coturnix coturnix japonica*) and white Pekin duck (*Anas platyrhynchos*) (AA Labs, Westminster, CA, USA) were incubated at 37°C until reaching HH9.5 (Fig. 5C). Embryos were handled following University and NIH guidelines. Unilateral grafts of anterior hindbrain and midbrain neural crest were excised from quail donors and transplanted into stage-matched duck hosts, producing chimeric 'quck' (Lwigale and Schneider, 2008; Schneider, 1999; Schneider and Helms, 2003).

Whole-mount Q¢PN immunohistochemistry

After ISH, embryos were post-fixed overnight in PFA, washed in PBS, blocked with 5% goat serum in PBS with 0.1% Triton X-100 for 1 hour and incubated with mouse anti-Q¢PN antibody (Developmental Studies Hybridoma Bank, University of Iowa) diluted 1:5 in block solution at 4°C overnight. Embryos were then washed in PBS and incubated with goat anti-mouse Alexa Fluor 488 (Jackson ImmunoResearch Laboratories) diluted 1:500 in block solution for 1 hour, washed in PBS and imaged.

Neural fold extirpation

Chick or duck embryos were incubated until HH9– (5 somites). The embryo was partially exposed by piercing the vitelline membrane, and the right side of dorsal neural fold from the posterior midbrain to the anterior hindbrain was extirpated using a tungsten needle (Fig. 6A). After surgery, tape was placed over the window, and embryos were returned to the incubator until collected for analysis.

Neural fold augmentation

Wild-type chick and transgenic GFP-chick (Crystal Bioscience, Emeryville, CA, USA) embryos were incubated until HH9– (5 somites). The embryo was partially exposed by piercing the vitelline membrane. The right side of the dorsal neural fold from transgenic GFP chicks was unilaterally extirpated and transferred to a wild-type chick embryo. An incision was made in the ectoderm lateral to the right side of the dorsal neural fold at the level of the posterior midbrain and anterior hindbrain. The isolated GFP+ dorsal neural fold was placed just lateral to the dorsal neural fold, above the mesoderm, at the site of the incision in the ectoderm (Fig. 6B). After surgery, tape was placed over the window, and embryos were returned to the incubator until collected for analysis.

Mandible size and symmetry quantification

Embryos were processed for differential skeletal staining as previously described (Eames and Schneider, 2008). After skeletal staining, mandibles were isolated and flat mounted in glycerol for imaging and quantification (Fig. 5J). The length of each side of the mandible (Fig. 5J, c) was calculated in Photoshop by drawing lines along the length of the mandible at the midline (Fig. 5J, a) and the width of the mandible at the most proximal edge of the bone (Fig. 5J, b).

Statistical methods

Unpaired Student's *t*-tests were used for comparisons of continuous variables between two groups. Two-tailed $P<0.05$ was considered statistically significant.

Acknowledgements

We thank K. Butcher for technical support; T. Alliston, S. Gline and E. Ealba for helpful discussions; and T. Dam at AA Lab Eggs for quail and duck eggs. The Q¢PN antibody was obtained from the DSHB maintained by the University of Iowa under auspices of the National Institute of Child Health and Human Development (NICHD).

Competing interests

The authors declare no competing financial interests.

Author contributions

R.A.S. and J.L.F. conceived the project; J.L.F., R.S.S. and K.C.W. performed the experiments; J.L.F., R.S.S. and K.C.W. compiled the data; R.A.S. and J.L.F. designed the experiments and analyzed the data; and R.A.S. and J.L.F. co-wrote the manuscript.

Funding

This work was funded by a Human Frontier Science Program Long-term Fellowship [LT-01061/2007-L]; and grants from the National Institute of Dental and Craniofacial Research (NIDCR) [F32 grant DE021929 to J.L.F.; R01 grant DE016402 to R.A.S.] and the National Institute of Child Health and Human Development (NICHD) [T32 grant HD007470 to K.C.W.]. Deposited in PMC for release after 12 months.

Supplementary material

Supplementary material available online at
http://dev.biologists.org/lookup/suppl/doi:10.1242/dev.100107/-/DC1

References

Ahlgren, S. C. and Bronner-Fraser, M. (1999). Inhibition of sonic hedgehog signaling in vivo results in craniofacial neural crest cell death. *Curr. Biol.* **9**, 1304-1314.
Allard, P. and Tabin, C. J. (2009). Achieving bilateral symmetry during vertebrate limb development. *Semin. Cell Dev. Biol.* **20**, 479-484.
Arthur, W. (1984). *Mechanisms of Morphological Evolution. A Combined Genetic, Developmental and Ecological Approach*. Hoboken, NJ: John Wiley & Sons Ltd.
Balczerski, B., Matsutani, M., Castillo, P., Osborne, N., Stainier, D. Y. and Crump, J. G. (2012). Analysis of sphingosine-1-phosphate signaling mutants reveals endodermal requirements for the growth but not dorsoventral patterning of jaw skeletal precursors. *Dev. Biol.* **362**, 230-241.
Basch, M. L., Bronner-Fraser, M. and García-Castro, M. I. (2006). Specification of the neural crest occurs during gastrulation and requires Pax7. *Nature* **441**, 218-222.
Betancur, P., Bronner-Fraser, M. and Sauka-Spengler, T. (2010). Assembling neural crest regulatory circuits into a gene regulatory network. *Annu. Rev. Cell Dev. Biol.* **26**, 581-603.
Betters, E., Liu, Y., Kjaeldgaard, A., Sundström, E. and García-Castro, M. I. (2010). Analysis of early human neural crest development. *Dev. Biol.* **344**, 578-592.
Brito, J. M., Teillet, M. A. and Le Douarin, N. M. (2006). An early role for sonic hedgehog from foregut endoderm in jaw development: ensuring neural crest cell survival. *Proc. Natl. Acad. Sci. USA* **103**, 11607-11612.
Brito, J. M., Teillet, M. A. and Le Douarin, N. M. (2008). Induction of mirror-image supernumerary jaws in chicken mandibular mesenchyme by Sonic Hedgehog-producing cells. *Development* **135**, 2311-2319.
Bronner-Fraser, M. (2008). On the trail of the 'new head' in Les Treilles. *Development* **135**, 2995-2999.
Coppinger, R. and Schneider, R. (1995). Evolution of working dogs. In *The Domestic Dog* (ed. J. Serpell), pp. 21-47. Cambridge: Cambridge University Press.
Couly, G. F., Coltey, P. M. and Le Douarin, N. M. (1993). The triple origin of skull in higher vertebrates: a study in quail-chick chimeras. *Development* **117**, 409-429.
Couly, G., Grapin-Botton, A., Coltey, P. and Le Douarin, N. M. (1996). The regeneration of the cephalic neural crest, a problem revisited: the regenerating cells originate from the contralateral or from the anterior and posterior neural fold. *Development* **122**, 3393-3407.
David, N. B., Saint-Etienne, L., Tsang, M., Schilling, T. F. and Rosa, F. M. (2002). Requirement for endoderm and FGF3 in ventral head skeleton formation. *Development* **129**, 4457-4468.
de Beer, G. (1940). *Embryos and Ancestors*. Oxford: Clarendon Press.
Depew, M. J. and Olsson, L. (2008). Symposium on the evolution and development of the vertebrate head. *J. Exp. Zool.* **310B**, 287-293.
Depew, M. J., Liu, J. K., Long, J. E., Presley, R., Meneses, J. J., Pedersen, R. A. and Rubenstein, J. L. (1999). Dlx5 regulates regional development of the branchial arches and sensory capsules. *Development* **126**, 3831-3846.
Depew, M. J., Lufkin, T. and Rubenstein, J. L. (2002). Specification of jaw subdivisions by Dlx genes. *Science* **298**, 381-385.
Dixon, J., Jones, N. C., Sandell, L. L., Jayasinghe, S. M., Crane, J., Rey, J. P., Dixon, M. J. and Trainor, P. A. (2006). Tcof1/Treacle is required for neural crest cell formation and proliferation deficiencies that cause craniofacial abnormalities. *Proc. Natl. Acad. Sci. USA* **103**, 13403-13408.
Duboule, D. (1994). Temporal colinearity and the phylotypic progression: a basis for the stability of a vertebrate Bauplan and the evolution of morphologies through heterochrony. *Dev. Suppl.* **1994**, 135-142.
Dutton, K. A., Pauliny, A., Lopes, S. S., Elworthy, S., Carney, T. J., Rauch, J., Geisler, R., Haffter, P. and Kelsh, R. N. (2001). Zebrafish colourless encodes sox10 and specifies non-ectomesenchymal neural crest fates. *Development* **128**, 4113-4125.

Ealba, E. L. and Schneider, R. A. (2013). A simple PCR-based strategy for estimating species-specific contributions in chimeras and xenografts. *Development* **140**, 3062-3068.
Eames, B. F. and Schneider, R. A. (2005). Quail-duck chimeras reveal spatiotemporal plasticity in molecular and histogenic programs of cranial feather development. *Development* **132**, 1499-1509.
Eames, B. F. and Schneider, R. A. (2008). The genesis of cartilage size and shape during development and evolution. *Development* **135**, 3947-3958.
Erwin, D. H. and Davidson, E. H. (2009). The evolution of hierarchical gene regulatory networks. *Nat. Rev. Genet.* **10**, 141-148.
Gilbert, S. F. (2010). *Developmental Biology*. Sunderland, MA: Sinauer Associates, Inc.
Glenn Northcutt, R. (2005). The new head hypothesis revisited. *J. Exp. Zool.* **304B**, 274-297.
Haldane, J. B. S. (1927). On being the right size. In *On Being the Right Size and Other Essays* (ed. J. Maynard-Smith), pp. 1-8. Oxford: Oxford University Press.
Hall, J., Jheon, A., Ealba, E. L., Eames, B. F., Butcher, K., Mak, S., Ladher, R., Alliston, T. and Schneider, R. A. (2013). Evolution of a developmental mechanism: Species-regulation of the cell cycle and the timing of events during craniofacial osteogenesis. *Dev. Biol.* doi: 10.1016/j.ydbio.2013.11.011.
Helms, J. A. and Brugmann, S. A. (2007). The origins of species-specific facial morphology: the proof is in the pigeon. *Integr. Comp. Biol.* **47**, 338-342.
Hunt, P., Ferretti, P., Krumlauf, R. and Thorogood, P. (1995). Restoration of normal Hox code and branchial arch morphogenesis after extensive deletion of hindbrain neural crest. *Dev. Biol.* **168**, 584-597.
Irie, N. and Kuratani, S. (2011). Comparative transcriptome analysis reveals vertebrate phylotypic period during organogenesis. *Nat. Commun.* **2**, 248.
Jeong, J., Mao, J., Tenzen, T., Kottmann, A. H. and McMahon, A. P. (2004). Hedgehog signaling in the neural crest cells regulates the patterning and growth of facial primordia. *Genes Dev.* **18**, 937-951.
Jeong, J., Li, X., McEvilly, R. J., Rosenfeld, M. G., Lufkin, T. and Rubenstein, J. L. (2008). Dlx genes pattern mammalian jaw primordium by regulating both lower jaw-specific and upper jaw-specific genetic programs. *Development* **135**, 2905-2916.
Jheon, A. H. and Schneider, R. A. (2009). The cells that fill the bill: neural crest and the evolution of craniofacial development. *J. Dent. Res.* **88**, 12-21.
Kalinka, A. T., Varga, K. M., Gerrard, D. T., Preibisch, S., Corcoran, D. L., Jarrells, J., Ohler, U., Bergman, C. M. and Tomancak, P. (2010). Gene expression divergence recapitulates the developmental hourglass model. *Nature* **468**, 811-814.
Klingenberg, C. P. (2011). MorphoJ: an integrated software package for geometric morphometrics. *Mol Ecol Resour* **11**, 353-357.
Köntges, G. and Lumsden, A. (1996). Rhombencephalic neural crest segmentation is preserved throughout craniofacial ontogeny. *Development* **122**, 3229-3242.
Kos, R., Reedy, M. V., Johnson, R. L. and Erickson, C. A. (2001). The winged-helix transcription factor FoxD3 is important for establishing the neural crest lineage and repressing melanogenesis in avian embryos. *Development* **128**, 1467-1479.
Kulesa, P., Bronner-Fraser, M. and Fraser, S. (2000). In ovo time-lapse analysis after dorsal neural tube ablation shows rerouting of chick hindbrain neural crest. *Development* **127**, 2843-2852.
LaBonne, C. and Bronner-Fraser, M. (2000). Snail-related transcriptional repressors are required in Xenopus for both the induction of the neural crest and its subsequent migration. *Dev. Biol.* **221**, 195-205.
Le Lièvre, C. S. and Le Douarin, N. M. (1975). Mesenchymal derivatives of the neural crest: analysis of chimaeric quail and chick embryos. *J. Embryol. Exp. Morphol.* **34**, 125-154.
Leevers, S. J. and McNeill, H. (2005). Controlling the size of organs and organisms. *Curr. Opin. Cell Biol.* **17**, 604-609.
Levin, M., Hashimshony, T., Wagner, F. and Yanai, I. (2012). Developmental milestones punctuate gene expression in the Caenorhabditis embryo. *Dev. Cell* **22**, 1101-1108.
Li, B., Kuriyama, S., Moreno, M. and Mayor, R. (2009). The posteriorizing gene Gbx2 is a direct target of Wnt signalling and the earliest factor in neural crest induction. *Development* **136**, 3267-3278.
Liu, B., Rooker, S. M. and Helms, J. A. (2010). Molecular control of facial morphology. *Semin. Cell Dev. Biol.* **21**, 309-313.
Livak K. J. and Schmittgen T. D. (2001). Analysis of relative gene expression data using real-time quantitative PCR and the $2^{-\Delta\Delta C(T)}$ method. *Methods* **25**, 402-408.
Lwigale, P. Y. and Schneider, R. A. (2008). Other chimeras: quail-duck and mouse-chick. *Methods Cell Biol.* **87**, 59-74.
Maczkowiak, F., Matéos, S., Wang, E., Roche, D., Harland, R. and Monsoro-Burq, A. H. (2010). The Pax3 and Pax7 paralogs cooperate in neural and neural crest patterning using distinct molecular mechanisms, in Xenopus laevis embryos. *Dev. Biol.* **340**, 381-396.
Martynoga, B., Morrison, H., Price, D. J. and Mason, J. O. (2005). Foxg1 is required for specification of ventral telencephalon and region-specific regulation of dorsal telencephalic precursor proliferation and apoptosis. *Dev. Biol.* **283**, 113-127.
Merrill, A. E., Eames, B. F., Weston, S. J., Heath, T. and Schneider, R. A. (2008). Mesenchyme-dependent BMP signaling directs the timing of mandibular osteogenesis. *Development* **135**, 1223-1234.
Mollaaghababa, R. and Pavan, W. J. (2003). The importance of having your SOX on: role of SOX10 in the development of neural crest-derived melanocytes and glia. *Oncogene* **22**, 3024-3034.
Murdoch, B., DelConte, C. and García-Castro, M. I. (2012). Pax7 lineage contributions to the mammalian neural crest. *PLoS ONE* **7**, e41089.
Nieto, M. A., Sargent, M. G., Wilkinson, D. G. and Cooke, J. (1994). Control of cell behavior during vertebrate development by Slug, a zinc finger gene. *Science* **264**, 835-839.
Nikitina, N., Sauka-Spengler, T. and Bronner-Fraser, M. (2008). Dissecting early regulatory relationships in the lamprey neural crest gene network. *Proc. Natl. Acad. Sci. USA* **105**, 20083-20088.
Noden, D. M. (1978). The control of avian cephalic neural crest cytodifferentiation. I. Skeletal and connective tissues. *Dev. Biol.* **67**, 296-312.
Noden, D. M. and Schneider, R. A. (2006). Neural crest cells and the community of plan for craniofacial development: historical debates and current perspectives. *Adv. Exp. Med. Biol.* **589**, 1-23.
Pikalow, A. S., Flynn, M. E. and Searls, R. L. (1994). Development of cranial flexure and Rathke's pouch in the chick embryo. *Anat. Rec.* **238**, 407-414.
Riedl, R. (1978). *Order in Living Organisms: Systems Analysis of Evolution.* Hoboken, NJ: John Wiley & Sons Ltd.
Roper, R. J., VanHorn, J. F., Cain, C. C. and Reeves, R. H. (2009). A neural crest deficit in Down syndrome mice is associated with deficient mitotic response to Sonic hedgehog. *Mech. Dev.* **126**, 212-219.
Rudolf, A. (1996). *The Shape of Life: Genes, Development, and the Evolution of Animal Form*. Chicago, IL: University of Chicago Press.
Sauka-Spengler, T. and Bronner-Fraser, M. (2008). A gene regulatory network orchestrates neural crest formation. *Nat. Rev. Mol. Cell Biol.* **9**, 557-568.
Scherson, T., Serbedzija, G., Fraser, S. and Bronner-Fraser, M. (1993). Regulative capacity of the cranial neural tube to form neural crest. *Development* **118**, 1049-1062.
Schneider, R. A. (1999). Neural crest can form cartilages normally derived from mesoderm during development of the avian head skeleton. *Dev. Biol.* **208**, 441-455.
Schneider, R. A. (2005). Developmental mechanisms facilitating the evolution of bills and quills. *J. Anat.* **207**, 563-573.
Schneider, R. A. and Helms, J. A. (2003). The cellular and molecular origins of beak morphology. *Science* **299**, 565-568.
Schneider, R. A., Hu, D. and Helms, J. A. (1999). From head to toe: conservation of molecular signals regulating limb and craniofacial morphogenesis. *Cell Tissue Res.* **296**, 103-109.
Sechrist, J., Nieto, M. A., Zamanian, R. T. and Bronner-Fraser, M. (1995). Regulative response of the cranial neural tube after neural fold ablation: spatiotemporal nature of neural crest regeneration and up-regulation of Slug. *Development* **121**, 4103-4115.
Shigetani, Y., Nobusada, Y. and Kuratani, S. (2000). Ectodermally derived FGF8 defines the maxillomandibular region in the early chick embryo: epithelial-mesenchymal interactions in the specification of the craniofacial ectomesenchyme. *Dev. Biol.* **228**, 73-85.
Siegenthaler, J. A., Tremper-Wells, B. A. and Miller, M. W. (2008). Foxg1 haploinsufficiency reduces the population of cortical intermediate progenitor cells: effect of increased p21 expression. *Cereb. Cortex* **18**, 1865-1875.
Steventon, B. and Mayor, R. (2012). Early neural crest induction requires an initial inhibition of Wnt signals. *Dev. Biol.* **365**, 196-207.
ten Berge, D., Brouwer, A., Korving, J., Reijnen, M. J., van Raaij, E. J., Verbeek, F., Gaffield, W. and Meijlink, F. (2001). Prx1 and Prx2 are upstream regulators of sonic hedgehog and control cell proliferation during mandibular arch morphogenesis. *Development* **128**, 2929-2938.
Teng, L., Mundell, N. A., Frist, A. Y., Wang, Q. and Labosky, P. A. (2008). Requirement for Foxd3 in the maintenance of neural crest progenitors. *Development* **135**, 1615-1624.
Tokita, M. and Schneider, R. A. (2009). Developmental origins of species-specific muscle pattern. *Dev. Biol.* **331**, 311-325.
Veitch, E., Begbie, J., Schilling, T. F., Smith, M. M. and Graham, A. (1999). Pharyngeal arch patterning in the absence of neural crest. *Curr. Biol.* **9**, 1481-1484.
von Baer, K. E. (1828). *Über Entwicklungsgeschichte der Thiere: Beobachtung und Reflexion*. Königsberg: Borntträger.
Withington, S., Beddington, R. and Cooke, J. (2001). Foregut endoderm is required at head process stages for anteriormost neural patterning in chick. *Development* **128**, 309-320.
Yardley, N. and García-Castro, M. I. (2012). FGF signaling transforms non-neural ectoderm into neural crest. *Dev. Biol.* **372**, 166-177.
Zelditch, M. (2004). *Geometric Morphometrics for Biologists: A Primer*. Amsterdam; Boston, MA: Elsevier Academic Press.